

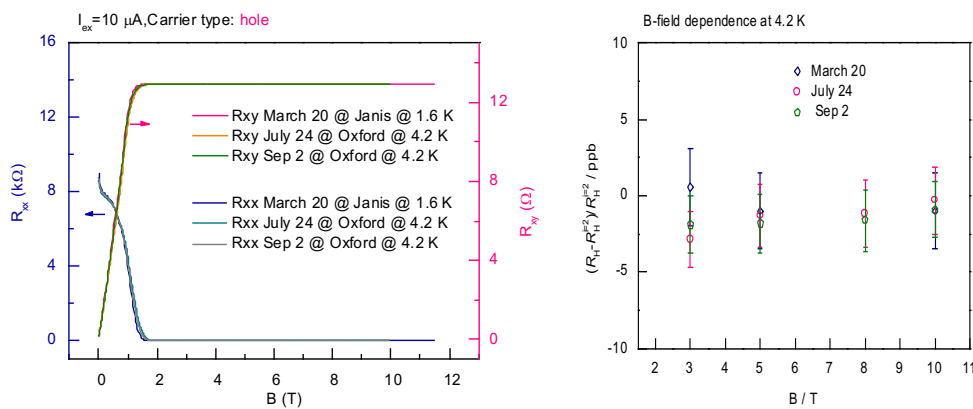
Progress Report of KRISS on DC, LF, RF and Magnetic Measurement (2019-2021)

DCLF: Hyung-Kew Lee (hyungkew.lee@kriss.re.kr)
RF: Jae-Yong Kwon (jykwon@kriss.re.kr)

1. Graphene QHR device (Dr. Jaesung Park, Dr. Dong-Hun Chae)

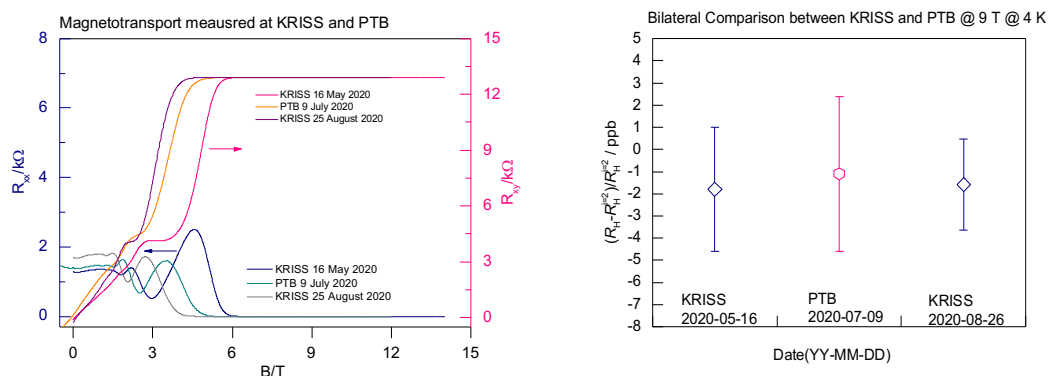
Study of long-term stability

Long-term stability of the graphene-based QHR is one of the problems that must be solved for replacing the GaAs-based QHR. We carried out precision measurement of the graphene QHR with capping layer in one year and found that the quantized values at the temperature of 4 K and above the magnetic field of 5 T are not changed within the measurement uncertainty. The graphene QHR device was kept in glove box with an inert environment when not being measured.



2. Bilateral Comparison of QHR in Graphene (Dr. Jaesung Park, Dr. Dong-Hun Chae)

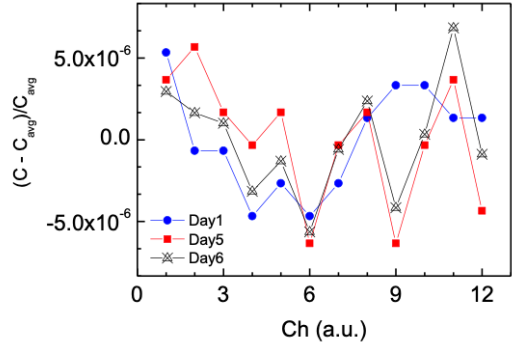
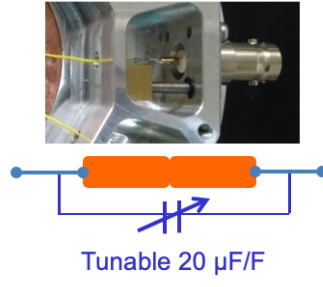
Bilateral comparison of quantum Hall resistance realized with a KRISS-made epitaxial graphene device was performed between PTB and KRISS. The device was delivered with an over-pressurized chamber made by KRISS by the standard airfreight. It turned out that the measured values are equivalent within the measurement uncertainty of a few parts per billion.



3. AC Voltage Ratio using PCD (Dr. Dan Bee Kim and Dr. Wan-Seop Kim)

The AC voltage ratio standard has been developed based on the concept of permuting capacitive device (PCD). 12 capacitors of 50 pF were selected to have similar capacitance values with each other, and their connection was

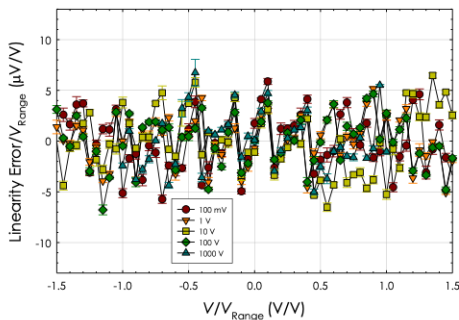
carefully designed to be symmetric. Furthermore, each capacitance was made to be adjustable within the range of 20 $\mu\text{F}/\text{F}$. Using the digitally assisted bridge and the PCD, the 10 : 1 AC voltage ratio of the ratio transformer has been calibrated, and the result agreed well with the value obtained by the Bootstrap method.



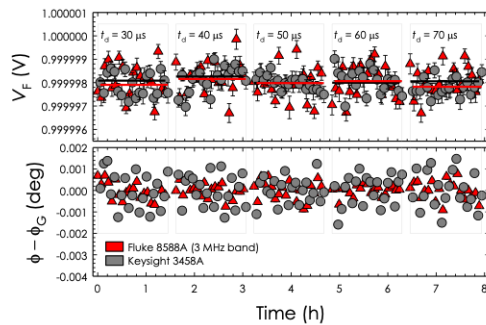
	In-phase	Quadrature
Bootstrap	9.999 999 8	0.000 000 2 rad
PCD	9.999 999 8	0.000 000 4 rad

4-1. Differential sampling based on a PJVS (Dr. Mun-Seok Kim)

- Effect of the sampler's bandwidth on differential sampling.
 - ✓ Keysight 3458A: $\Delta f \sim 150 \text{ kHz}$, $\Delta V_{\text{err}} \approx -25 \mu\text{V}/\text{V}$ at 1 kHz
 - ✓ NI-PXI-5922: $\Delta f \gg 1 \text{ MHz}$, $\Delta V_{\text{err}} \approx 0$ at least within the frequency range of kilohertz
- *Measurement configurations for differential sampling of AC waveforms based on a programmable Josephson voltage standard: effects of sampler bandwidth on the measurements (Mun-Seog Kim et al., Metrologia, 2020)
- An alternative sampler: **Fluke 8588A**.
 - ✓ Band width of low-pass filter: 3 MHz



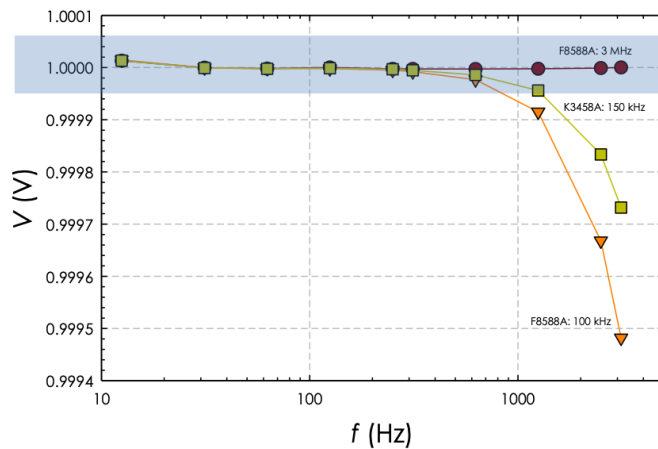
Linearity evaluation: $\sim 5 \mu\text{V}/\text{V}$ for all the ranges



Comparison at 62.5 Hz (Fluke 8588A and Keysight 3458A): Difference 92 nV with type A uncertainty of approximately 200 nV.

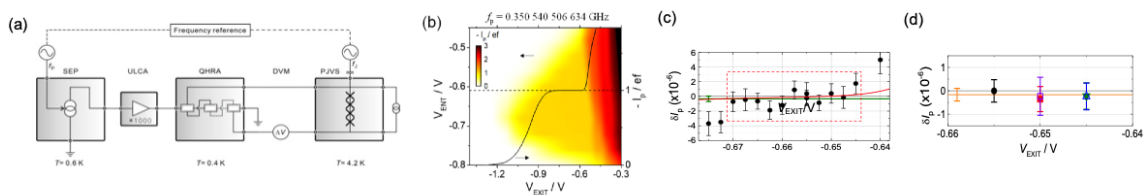
4-2. Differential sampling based on a PJVS (Dr. Mun-Seok Kim)

1 V Differential Measurement: Keysight 3458A/Fluke 8588A



For Fluke 8588A, the bandwidth effect on the differential sampling up to 3 kHz can be negligible.

5. Precision measurement of single-electron current with quantized Hall array resistance and Josephson voltage (Myung-Ho Bae, Dong-Hun Chae, Mun-Seog Kim, Bum-Kyu Kim, Nam Kim, Wan-Seop Kim)



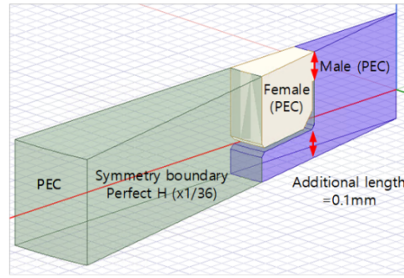
(a) Experimental scheme for the SEP precision measurement. (b) Pump-current map as a function of two gate voltages, V_{ENT} and V_{EXIT} at $f_p = 0.35$ GHz ($T = 0.55$ K, $B = 12$ T). Black curve: $-I_p/ef_p$ as a function of V_{EXIT} at $V_{ENT} = -0.61$ V, which shows a current plateau at $-I_p/ef_p = 1$ ($ef_p = 56.162\,780\,9$ pA). (c) Precision measurement results, $\delta I_p [= (-I_p - ef_p)/ef_p]$, for varying V_{EXIT} on the first current plateau in (b). Each data point was taken for ~ 49 min. The data in the dashed box show a plateau region with an average deviation (horizontal green line) and a type-A uncertainty (green error bar), $\delta I_p \pm u_A = (-0.33 \pm 0.37) \times 10^{-6}$. (d) The deviations with combined uncertainties (u_r , $k = 1$) obtained at three V_{EXIT} values for four different thermal cycles. The average deviation with u_r for the five points in (d) including the average data in (c) is $(-0.17 \pm 0.27) \times 10^{-6}$, as indicated by the orange horizontal line with an error bar (a total averaging time ~ 36 h).

6. RF Impedance (Dr. Chi-Hyun Cho)

A temporary team has been formed to prepare the 2.4 mm coaxial impedance KC. We are making a new attempt to collaborate with several researchers, not individually responsible for the key quantity. The new team worked to design proper airline length and jig, analyze connector effect analysis, and improve calibration service. COVID-19 has delayed the purchase of new airlines, but it is expected that new impedance standard will be prepared soon.



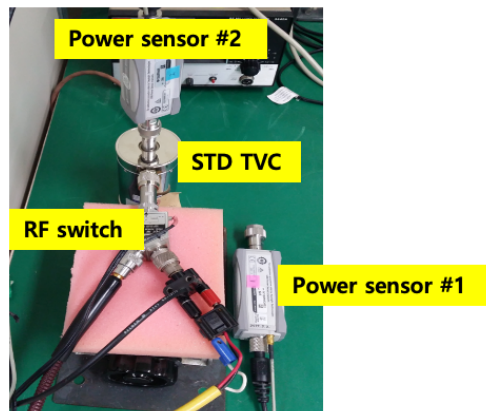
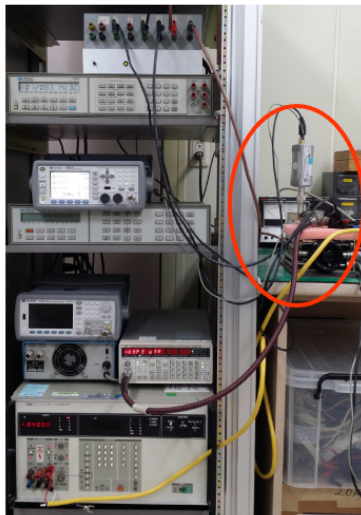
New Zig for airline measurement



Connector effect analysis

7-1. RF power (Dr. Tae-Weon Kang, Mr. Jeong-II Park)

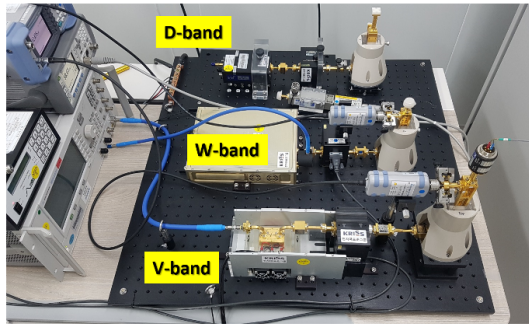
Frequency range of the power standards was extended down to 1 kHz. To measure the effective efficiency of thermoelectric power sensors (PSs) in the low-frequency range a reference thermal voltage converter (TVC) is employed. A modified RF voltage measurement system enables us to transfer the RF voltage standard of the TVC to the PS. Comparing the RF power to DC substituted power of the PS gives the effective efficiency. Evaluated expanded uncertainty is 1.7 % ($k = 2$) in the frequency range of 1 kHz to 1 MHz.



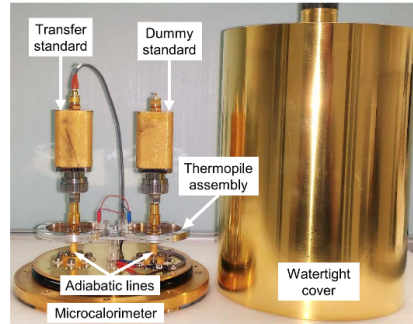
Power sensor calibration system using a TVC

7-2. RF power (Dr. Jae-Yong Kwon)

The improvement of V-/W-/D-band (50 GHz ~ 170 GHz) waveguide power calibration system was finalized. We are planning to open domestic RF power calibration services in V-/W-band in 2021. KRISS-CENAM collaborated to establish a 2.4-mm coaxial microcalorimeter system. KRISS designed and fabricated the system for evaluation. (IEEE TIM 2020)



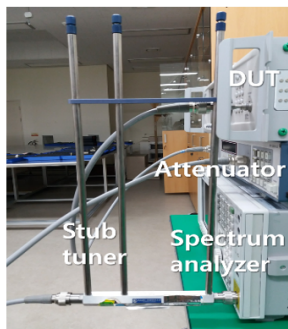
V-/W-/D-band waveguide direct comparison system



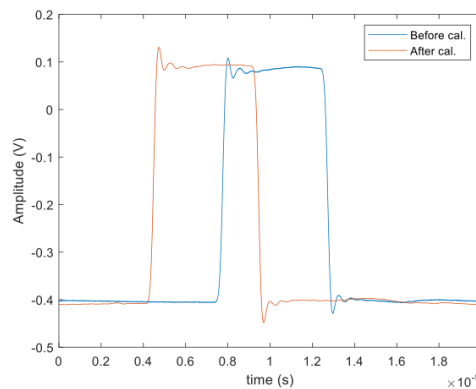
2.4-mm coaxial microcalorimeter at CENAM ¹⁰

8. Pulse Parameters (Dr. Chi-Hyun Cho, Dr. Joo-Gwang Lee)

Pulse waveform metrology based on electro-optic sampling was started since 2013. The calibration methods for real-time and sampling oscilloscopes have been developed, and traceability for time domain waveform measurements has been established. In this year, we launched services for AM, FM, PM analog modulation index and rise/fall time measurement.



Analog modulating index measurement system



Corrected waveform in time-domain

11

9. Field strength (Dr. Young-Pyo Hong)

We have developed a standard field generation system with an antenna for the calibration of a Ka-band (26.5 ~ 40 GHz) electric-field probe. The system has the unique capability of field measurements not only while rotating the azimuth angle of an electric-field strength measuring probe but also while changing the separation distance between the antenna and the probe. An evaluation of the uncertainty of the components providing traceability to the system was also conducted.

